Controllable Synthesis of Metal–Organic Frameworks: From MOF Nanorods to Oriented MOF Membranes

By *Yan-Shuo Li,* Helge Bux, Armin Feldhoff,* Guo-Ling Li, Wei-Shen Yang,* and *Jürgen Caro*

In recent years metal–organic frameworks (MOFs) have emerged as an intriguing class of hybrid nanoporous crystalline materials as a result of their highly diversified framework topologies and tailorable organic functionality.[1] They have shown promising applications for hydrogen storage,[1b] gas separation,[1e] catalysis,[1f] molecular recognition,[1g] and, more recently, as proton exchange membranes for high temperature fuel cells.[1h] Recently, MOF thin films has been attracting particular attention for use as smart membranes, catalytic coatings, chemical sensors, and related nanodevices.[2] As in the related research on zeolite thin films, morphology control is an important issue when manipulating MOF materials as molecular sieve membranes. Accordingly, two challenges present themselves: i) the preparation of size- and shape-controlled MOF nanocrystals and ii) the optimization of film microstructures, including grain size and shape, grain boundaries, and channel orientations. Stabilizing agents,[3] coordination modulators[4] or specific synthetic techniques, such as microwave heating,[5] ultrasonic synthesis,[6] and microemulsion methods,[7] have been used in the attempt to achieve size and shape control of MOF nanocrystals. Organic self-assembled monolayers (SAMs) were used to detect the assembly of secondary building units (SBUs) so as to control the surface deposition of MOF thin films.[8] Stepwise layer-by-layer growth of MOF thin films was introduced by Fischer and coworkers, and shown to offer better control over the film thickness and orientation.[9] Zeolitic imidazolate framework ZIF-7 ($Zn(bim)_2$) with sodalite (SOD) topology is formed by bridging benzimidazolate (bim) anions and zinc cations, exhibiting a hexagonal space group ($R\bar{3}$).[10] Two types of hexagonal faces are included in the sodalite cages of ZIF-7 (see Figure S1 in the Supporting Information): two normal hexagonal windows (perpendicular to the <001> axes, around 0.3 nm) and six distorted ones (perpendicular to the <1$\bar{1}\bar{1}$> axes, approximately 0.35 nm × 0.20 nm). This multidimensional and anisotropic channel network makes ZIF-7 an excellent model system for fundamental studies on achieving crystallographic preferred orientation (CPO) in MOF films and investigating its effect on permeation properties, as in the case of MFI zeolite membranes.[11] In this Communication, we report a recent advance in the control of size and shape in the synthesis of ZIF-7 nanocrystals, and the orientation modulation of ZIF-7 membranes based on evolutionary selection (van der Drifts growth) model.[12] The resulting oriented ZIF-7 membrane is evaluated in H_2/CO_2 mixture gas separation using the Wicke–Kallenbach technique.

Using a modified synthetic protocol after the original report of Yaghi and coworkers,[10b] we synthesized ZIF-7 nanoparticles at room temperature from a solution containing excess bim.[2j] **Figure 1a** shows the transmission electron microscopy (TEM) image of the ZIF-7 nanoparticles. The average particle size is 30.7 ± 5.9 nm (Figure 1b). The high-resolution TEM (HRTEM) image in Figure 1c shows the lattice fringes for a ZIF-7 nanocrystal. The particle with hexagonal shape appears to be a single-crystal domain with high crystallinity and exhibits a 1.15 nm *d*-spacing for the (1 1 0) lattice fringes. The selected area electron diffraction (SAED) pattern from a circular area 1.2 μm in diameter shows six Debye–Scherrer rings (Figure 1d). The 110 reflection is the most intense ring, followed by the $\bar{1}$32 and 312 reflections.

In our previous work, the purified ZIF-7 nanoparticles were re-dispersed into a polyethyleneimine (PEI) solution to obtain a viscous seeding solution.[2j,k] PEI was used to enhance the linkage between the seeds and the support. Here, we report a "one-pot" synthesis strategy that combines these two steps: zinc nitrate and bim at stoichiometric ratio (molar ratio 1:2) were directly dissolved into a PEI-dimethylfomamide (DMF) solution at room temperature. The obtained colloidal solution can be directly used as a seeding sol for the membrane fabrication. By altering the molar ratio of PEI and the reaction duration we can adjust the size of the ZIF-7 nanoparticles from 40 nm to 140 nm, as shown in **Figure 2**. All the products are single-phase ZIF-7 materials as characterized by powder X-ray diffraction (PXRD) (see Figure S2). Some hexagonal features become distinguishable in the case of ZIF-7@PEI-3#. PEI has a high density of amino groups, therefore it can act as a base to deprotonate bim, allowing the quick generation of a large number of ZIF-7 nuclei at the early stage of crystallization, which is critical for the synthesis of nanocrystals.

The aspect ratio, that is, the ratio of the average crystal length to the average crystal width, is the most important factor in determining the CPO of the deposited films according to evolutionary selection (van der Drift growth) model. If the influence of solvent molecules is neglected, the aspect ratio of ZIF-7

[*] Prof. Y.-S. Li, H. Bux, Dr. A. Feldhoff, Prof. J. Caro
Institute of Physical Chemistry and Electrochemistry, and the Laboratory for Nano and Quantum Engineering (LNQE) in cooperation with the Center for Solid State Research and New Materials
Leibniz University Hannover
Callinstrasse 3A, 30167 Hannover (Germany)
E-mail: leeys@dicp.ac.cn; armin.feldhoff@pci.uni-hannover.de
Prof. Y.-S. Li, G.-L. Li, Prof. W.-S. Yang
State Key Laboratory of Catalysis
Dalian Institute of Chemical Physics
Chinese Academy of Sciences
Zhong-Shan Road 457, 116023 Dalian (P. R. China)

DOI: 10.1002/adma.201000857

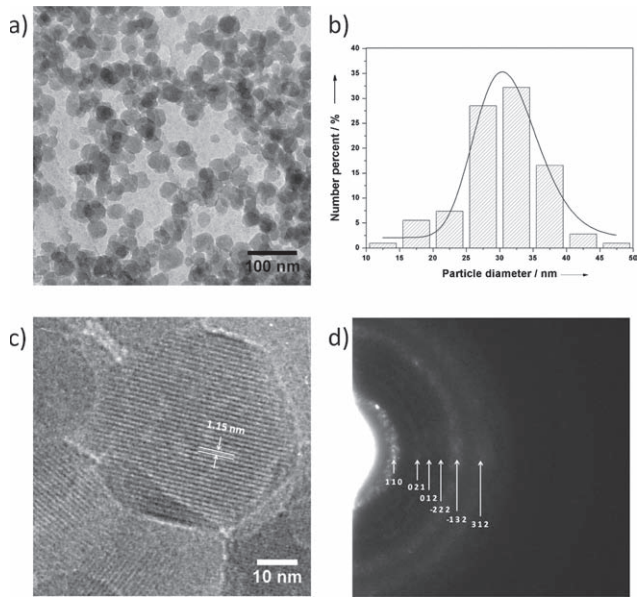

Figure 1. a) TEM bright-field image and b) particle size distribution of the ZIF-7 nanocrystals prepared by the excess ligand method. c) HRTEM image of the ZIF-7 nanocrystals, which shows a *d*-spacing of 1.15 nm for the (110) lattice plane. d) SAED pattern from a circular area 1.2 μm in diameter.

crystals is predicted to be close to 1 using the surface energy method (E_{sur}, see Table S1), that is, equilibrium morphology. This low aspect ratio also accounts for the random orientation of the ZIF-7 membrane which was seeded grown from the same synthesis system.[2j,k] The growth rates of the low index faces were also analyzed by calculating the attachment energies (E_{att}, see Table S1) using the Hartman–Perdok method (periodic bond chain (PBC) theory).[13] Among the low index planes, the {003} planes belong to kinked (K) faces, having the highest E_{att}, and therefore grow fastest; {110} and {101} planes belong to flat (F) faces, having the lowest E_{att}, and will be the most dominant faces in the final crystals. In the present study, we used $ZnCl_2$ instead of $Zn(NO_3)_2{\cdot}6H_2O$ as the zinc source. According to the hard soft acid base (HSAB) theory,[14] both chloride and zinc are classified as "intermediate", indicating a strong interaction between them. Therefore, the existence of chloride ions will have a great influence on the growth kinetics of ZIF-7 crystals, and result in an enlarged difference between the growth rates of {003} and {110}, {101} faces. In fact, a strong effect of anions (especially the halide anions) on the shape control of crystalline complexes or coordination polymers has been widely observed.[15] All the ZIF-7 crystals synthesized with $ZnCl_2$ exhibited prismatic hexagonal shapes with high aspect ratios, whether microwave heating (**Figures 3a**,**b**) or conventional heating (Figures 3c,d) was used. Owing to the rapid and volumetric dielectric heating, the microwave-synthesized ZIF-7 crystals are much smaller than the ones synthesized with conventional heating, implying a higher nucleation rate in the former case. The sizes and aspect ratios of the ZIF-7 crystals can be adjusted by altering the amount of diethylamine (DEA) that is added as deprotonating agent. It is suspected that the distributions of the precursor species, such as the Zn-bim primary complexes, can be adjusted by control of the deprotonation degree of the linker (bim), and which in turn has an

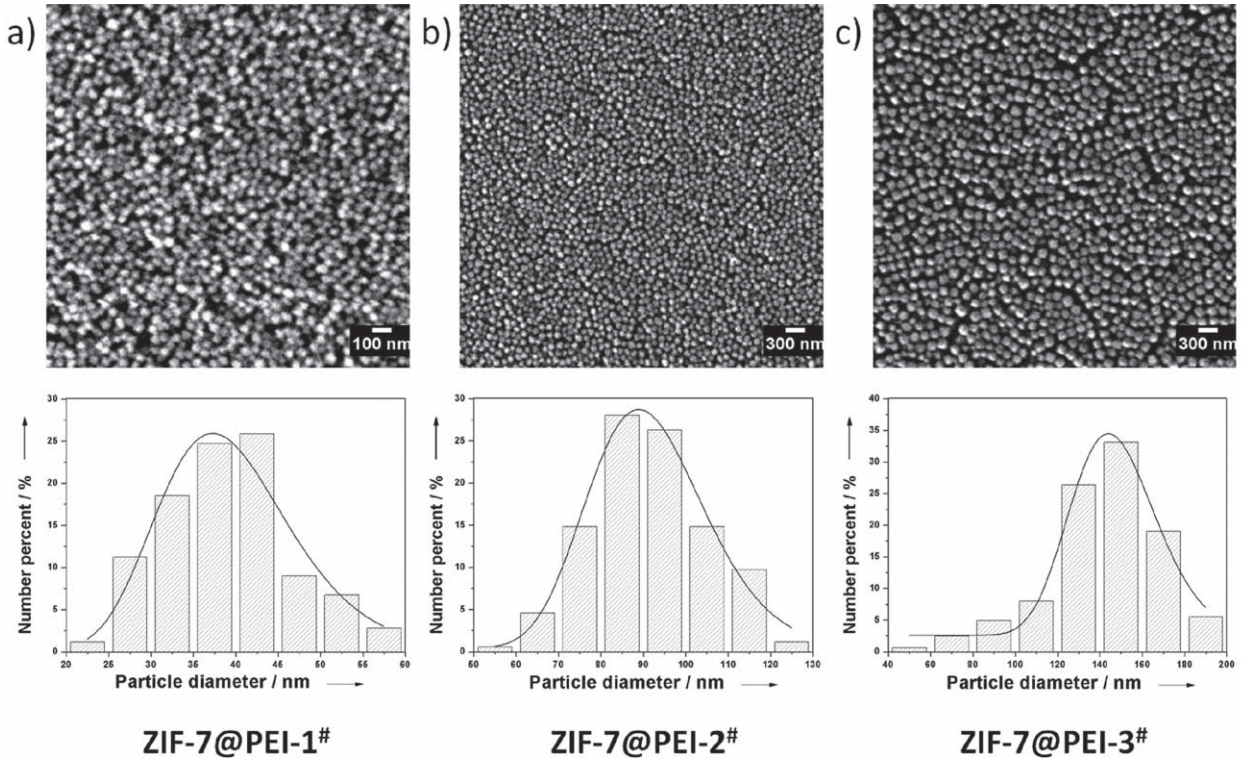

Figure 2. SEM images of the ZIF-7 nanoparticles synthesized by the "one-pot" method. Size distributions were determined by image analysis.

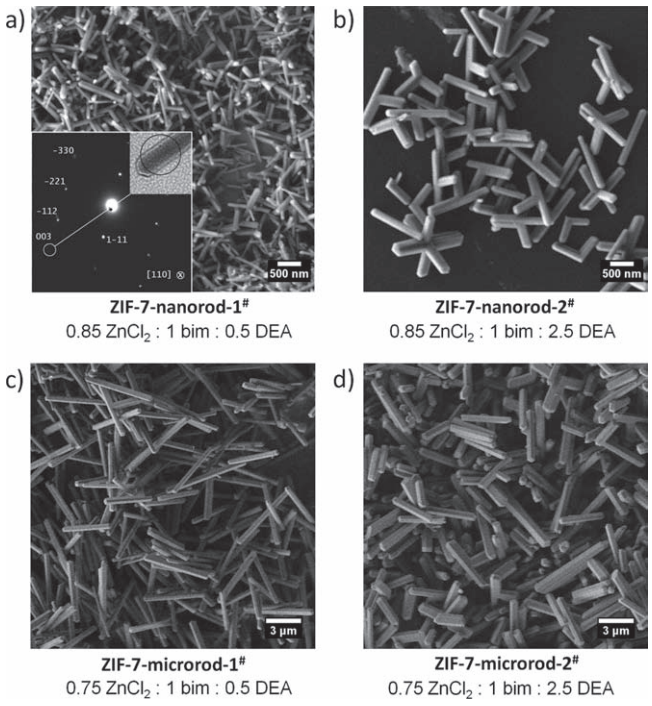

Figure 3. a–d) SEM images of the ZIF-7 nanorods and microrods. Inset in (a): Typical SAED pattern from a single nanorod (ZIF-7-nanorod-1#), verifying that the long axis of the rod-shaped crystal is parallel to the *c*-axis. The image descriptions give the molar ratios in the synthesis solutions.

influence on the growth kinetics. It is also notable that simultaneously parallel twins or intergrown twins can be observed in the case of microwave synthesis (Figures 3a,b). The reason for this high density of twins under microwave irradiation is still unknown. The SAED pattern (inset, Figure 3a) of ZIF-7-nanorod-1# demonstrates that the nanorod shown in the TEM bright-field image (inset, Figure 3a) is oriented almost along the [110] zone axis, and the longitudinal axis of the nanorod is along the *c*-axis.

In light of these morphology control studies, manipulation of the CPO of ZIF-7 membranes was attempted through evolutionary selection in a van der Drift–type growth. The nearly spherical shape of the seeding crystals (ZIF-7@PEI-2#) resulted in a randomly oriented seed layer (see Figure 2b and **Figure 4d**). Deviation from random orientation appeared after 45 min of microwave assisted secondary growth (Figure 4a). Nevertheless, the CPO distribution is broad and a very vague maximum develops at about 15°–45°. The *c*-out-of-plane orientation was significantly manifested with extended secondary growth time (Figure 4b,c); the CPO distribution became narrower and the maximum shifted to 10°. The membrane thickness increased nearly linearly with synthesis time, indicating the absence of further nucleation. The columnar grains growing from the seed layer became thicker when secondary growth was prolonged from 45 min to 225 min (Figures 4a–c). Unlike the microwave synthesis of ZIF-7 nanorods, twins were seldom observed during the microwave-assisted secondary growth, which indicates that in the former case the twinning might occur during the nucleation stage. The 030, 110, and 220 peaks are weak for the oriented membranes, indicating that these planes are almost vertical to the substrate surface. Instead of a completely *c*-out-of-plane orientation, the ZIF-7 membranes showed an enhancement of the relative intensities of the 101, 202, 303, 012, 132, and 113 reflections with increasing secondary growth time according to the XRD characterizations (Figure 4d). It is notable that this oblique CPO should not be described as 101 CPO, but can be well explained by refined evolutionary selection in a van der Drift–type growth, taking into consideration both the fastest growth direction and the lateral growth component.[16]

The *c*-out-of-plane oriented ZIF-7 membrane (Figure 4c) was tested for H_2/CO_2 equimolar gas mixture separation using the Wicke-Kallenbach technique with gas chromatographic control.[2j,k] Similar to our previous report on randomly oriented ZIF-7 membrane, the oriented membrane (Figure 4c) exhibited an increase in selectivity with temperature. A H_2/CO_2 mixture separation factor of 8.4 was measured at 200 °C (see Figure S3), which is much larger than the Knudsen separation factor of 4.7. However, the H_2 permeance of the oriented membrane was one-tenth that of the randomly oriented membrane. This observation is understandable considering the anisotropic pore structure of ZIF-7 crystals. Neither the pyramidal termination {101} faces nor the prismatic {110} faces of the columnar crystals possess direct entrances (the hexagonal windows) for guest molecules (see Figure S1). This feature might result in so-called surface resistance and the grain boundary resistance associated with the mass transport through polycrystalline separating layers,[17] which account for the lower permeance of the *c*-out-of-plane ZIF-7 membrane. Morphology-dependent gas adsorption of coordination polymers has been reported by different researchers.[18] In the next study, we will attempt to correlate the membrane performances with both the kinetics and equilibrium of H_2 adsorption on the ZIF-7 crystals with different sizes and morphologies.

In summary, supramolecular assembly methods have been developed for the fabrication of highly oriented MOF thin films.[8,9] A general and effective solvothermal route is introduced in the present work to tailor the crystal size and morphology of MOF materials and to manipulate the orientation of MOF films through evolutionary selection in a van der Drift–type growth originating from randomly oriented seed layers. A microstructure-related membrane performance of ZIF-7 membranes was observed, which has been extensively studied in the field of zeolite membranes,[11] and should also be an important issue in the development of high-quality MOF membranes. Besides this, when targeting the applications of MOF thin films in catalytic coatings, chemical sensors, and related advanced nanodevices, it will also be of great significance and a big challenge to manipulate the channel orientation and grain morphology of the MOF films.

Experimental Section

Synthesis of ZIF-7 Nanoparticles: ZIF-7 nanoparticles were synthesized according to our previous report.[2j] For the "one-pot" synthesis of ZIF-7@PEI colloids, a given amount (0.140 g, 0.140 g, and 0.360 g for ZIF-7@PEI-1#, ZIF-7@PEI-2#, and ZIF-7@PEI-3#, respectively) of branched PEI (average M_w ~25000) was dissolved in DMF (200 mL). $Zn(NO_3)_2{\cdot}6H_2O$ (0.446 g) and benzimidazole (0.354 g) were directly mixed into this solution at room temperature. After being kept at room temperature for a certain period (5 h, 24 h, and 1 h for ZIF-7@PEI-1#, ZIF-7@PEI-2#, and

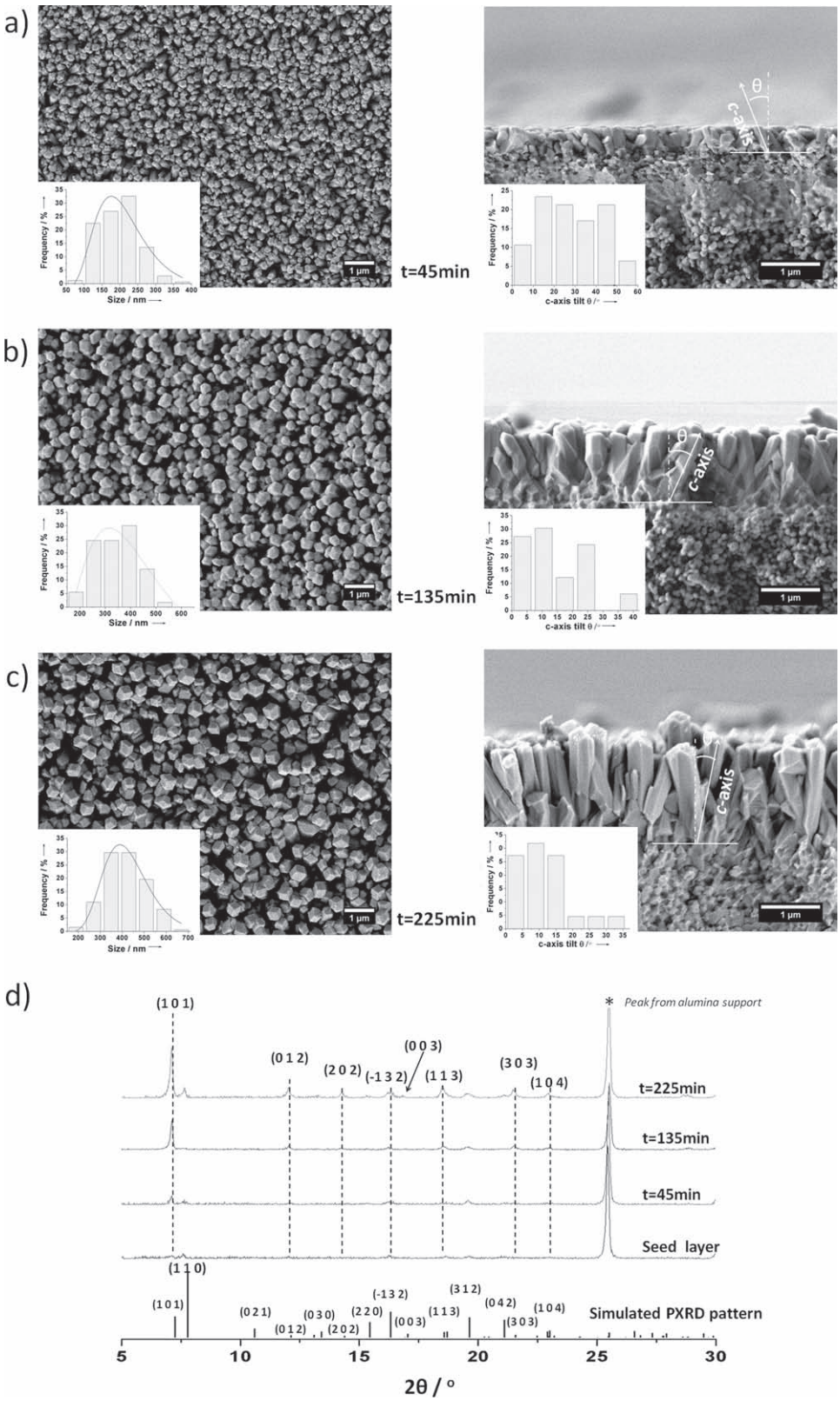

Figure 4. SEM top views and cross sections of the ZIF-7 membranes obtained after different times of microwave assisted secondary growth: a) 45 min, b) 135 min, and c) 225 min. d) the XRD patterns of the ZIF-7 membranes and the simulated PXRD pattern of ZIF-7 crystal. Insets in the SEM top views give the distributions of the cross-sectional size of the columnar crystals, and the CPO distributions. The CPO is represented by the angle θ between *c*-axis and the substrate normal.

ZIF-7@PEI-3#, respectively), the product was centrifugally concentrated to a volume of around 9 mL, containing around 2.5 wt% ZIF-7, assuming a yield of 50%.

Synthesis of ZIF-7 Nanorods and Microrods: DMF (30 mL) was added to a solid mixture of $ZnCl_2$ (0.295 g for nanorods or 0.265 g for microrods) and benzimidazole (0.310 g), and a given amount of diethylamine (0.093 g or 0.465 g) was added. The solvothermal synthesis was carried out in a microwave oven (Ethos 1, MLS) at 100 °C for 90 min (nanorods) or in an air oven at 130 °C for 24 h (microrods). The products were centrifuged and washed with ethanol.

Preparation of Oriented ZIF-7 Membranes: An asymmetric alumina disc (Inocermic) was surface seeded by dip-coating in the ZIF-7@PEI-2# colloid for 20 s. For the secondary growth, 30 mL DMF was added to a solid mixture of $ZnCl_2$ (0.204 g) and benzimidazole (0.266 g), and diethylamine (0.170 g) was added. The clear solution was transferred into a poly(tetrafluoroethylene) (Teflon) autoclave in which the seeded support was placed vertically. Afterwards the autoclave was heated in a microwave oven (Ethos 1, MLS) at 100 °C for a certain period. After cooling down, the membrane was washed with methanol.

It should be noted that to guarantee a high reproducibility the anhydrous chemical reagents used for the synthesis should be handled carefully to avoid deliquescence or moisture sorption.

Experimental characterization techniques, including XRD, SEM, SAED, and HRTEM, as well as permeation measurements are described in detail in the Supporting Information.

Supporting Information

Supporting Information is available online from Wiley InterScience or from the authors.

Acknowledgements

Y.-S. Li thanks the Alexander von Humboldt Foundation for financial support and Prof. Wei-Xue Li for valuable discussion. DFG Priority Program 1362 "Porous Metal-Organic Frameworks" is thanked for financial support.

Received: March 10, 2010
Revised: March 30, 2010
Published online: June 8, 2010

[1] a) S. Kitagawa, R. Kitaura, S. Noro, *Angew. Chem. Int. Ed.* **2004**, *43*, 2334; b) M. Yaghi, M. O'Keeffe, N. W. Ockwig, H. K. Chae, M. Eddaoudi, J. Kim, *Nature* **2003**, *423*, 705; c) G. Ferey, *Chem. Soc. Rev.* **2008**, *37*, 191; d) S. L. James, *Chem. Soc. Rev.* **2003**, *32*, 276; e) J.-R. Li, R. J. Kuppler, H.-C. Zhou, *Chem. Soc. Rev.* **2009**, *38*, 1477; f) J. Lee, O. K. Farha, J. Roberts, K. A. Scheidt, S. T. Nguyen, J. T. Hupp, *Chem. Soc. Rev.* **2009**, *38*, 1450; g) X. D. Chen, C. Q. Wan, H. H. Y. Sung, I. D. Williams, T. C. W. Mak, *Chem. Eur. J.* **2009**, *15*, 6518; h) J. A. Hurd, R. Vaidhyanathan, V. Thangadurai, C. I. Ratcliffe, I. L. Moudrakovski, G. K. H. Shimizu, *Nat. Chem.* **2009**, *1*, 705.

[2] a) D. Zacher, O. Shekhah, C. Wöll, R. A. Fischer, *Chem. Soc. Rev.* **2009**, *38*, 1418; b) M. Arnold, P. Kortunov, D. J. Jones, Y. Nedellec, J. Kärger, J. Caro, *Eur. J. Inorg. Chem.* **2007**, *1*, 60; c) Y. Yoo, H. K. Jeong, *Chem. Commun.* **2008**, 2441; d) J. Gascon, S. Aguado, F. Kapteijn, *Microporous Mesoporous Mater.* **2008**, *113*, 132; e) Y. Liu, Z. Ng, E. A. Khan, H. K. Jeong, C. Ching, Z. P. Lai, *Microporous Mesoporous Mater.* **2009**, *118*, 296; f) Y. Yoo, Z.-P. Lai, H. K. Jeong, *Microporous Mesoporous Mater.* **2009**, *123*, 100; g) H. Guo, G. Zhu, I. J. Hewitt, S. L. Qiu, *J. Am. Chem. Soc.* **2009**, *131*, 1646; h) R. Ranjan, M. Tsapatsis, *Chem. Mater.* **2009**, *21*, 4920; i) H. Bux, F. Y. Liang, Y. S. Li, J. Cravillon, M. Wiebcke, J. Caro, *J. Am. Chem. Soc.* **2009**, *131*, 16000; j) Y. S. Li, F. Y. Liang, H. Bux, A. Feldhoff, W. S. Yang, J. Caro, *Angew. Chem. Int. Ed.* **2010**, *49*, 548; k) Y. S. Li, F. Y. Liang, H. Bux, W. S. Yang, J. Caro, *J. Membr. Sci.* **2010**, *354*, 48.

[3] S. Hemes, T. Witte, T. Hitov, D. Zacher, S. Bahnmueller, G. Langstein, K. Huber, R. A. Fischer, *J. Am. Chem. Soc.* **2009**, *126*, 5324.

[4] T. Tsuruoka, S. Furukawa, Y. Takashima, K. Yoshida, S. Isoda, S. Kitagawa, *Angew. Chem. Int. Ed.* **2009**, *48*, 4739.

[5] Z. Ni, R. I. Masel, *J. Am. Chem. Soc.* **2006**, *128*, 12394.

[6] Z. Q. Li, L. G. Qiu, T. Xu, Y. Wu, W. Wang, Z. Y. Wu, X. Jiang, *Mater. Lett.* **2009**, *63*, 78.

[7] K. M. L. Taylor, W. J. Rieter, W. B. Lin, *J. Am. Chem. Soc.* **2008**, *130*, 14358.

[8] a) E. Biemmi, C. Scherb, T. Bein, *J. Am. Chem. Soc.* **2007**, *129*, 8054; b) S. Hermes, F. Schröder, R. Chelmowski, C. Wöll, R. A. Fischer, *J. Am. Chem. Soc.* **2005**, *127*, 13744.

[9] a) O. Shekhah, H. Wang, S. Kowarik, F. Schreiber, M. Paulus, M. Tolan, C. Sternemann, F. Evers, D. Zacher, R. A. Fischer, C. Wöll, *J. Am. Chem. Soc* **2007**, *129*, 15118; b) O. Shekhah, H. Wang, T. Strunskus, P. Cyganik, D. Zacher, R. A. Fischer, C. Wöll, *Langmuir* **2006**, *23*, 7740.

[10] a) X. C. Huang, J. P. Zhang, X. M. Chen, *Chin. Sci. Bull.* **2003**, *48*, 1531; b) K. S. Park, Z. Ni, A. P. Côté, J. Y. Choi, R. Huang, F. J. Uribe-Romo, H. K. Chae, M. O'Keeffe, O. M. Yaghi, *Proc. Natl. Acad. Sci. USA* **2006**, *103*, 10186.

[11] a) Z. P. Lai, G. Bonilla, I. Diaz, J. G. Nery, K. Sujaoti, M. A. Amat, E. Kokkoli, O. Terasaki, R. W. Thompson, M. Tsapatsis, D. G. Vlachos, *Science* **2003**, *300*, 456; b) M. A. Snyder, M. Tsapatsis, *Angew. Chem. Int. Ed.* **2007**, *46*, 7560.

[12] A. Van Der Drift, *Philips Res. Rep.* **1967**, *22*, 267.

[13] P. Hartman, W. Perdok, *Acta Crystallogr.* **1955**, *8*, 521.

[14] R. G. Pearson, *J. Am. Chem. Soc.* **1963**, *85*, 3533.

[15] a) M. A. Withersby, A. J. Blake, N. R. Champness, P. Hubberstey, W. S. Li, M. Schröder, *Angew. Chem., Int. Ed.* **1997**, *36*, 2327; b) N. R. Brooks, A. J. Blake, N. R. Champness, J. W. Cunningham, P. Hubberstey, S. J. Teat, C. Wilson, M. Schröder, *J. Chem. Soc., Dalton Trans.* **2001**, 2530.

[16] A. J. Bons, P. D. Bons, *Microporous Mesoporous Mater.* **2003**, *62*, 9.

[17] a) D. A. Newsome, D. S. Sholl, *J. Phys. Chem. B* **2005**, *109*, 7237; b) A. Feldhoff, J. Caro, H. Jobic, J. Ollivier, C. B. Krause, P. Galvosas, J. Kärger, *ChemPhysChem* **2009**, *10*, 2429.

[18] a) H. J. Lee, W. Cho, S. Jung, M. Oh, *Adv. Mater.* **2008**, *21*, 674; b) T. Tsuruoka, S. Furukawa, Y. Takashima, K. Yoshida, S. Isoda, S. Kitagawa, *Angew. Chem. Int. Ed.* **2009**, *48*, 4739.